Supplementary Information for:

Global patterns and drivers of C:N:P in marine ecosystems

Tatsuro Tanioka[1], Catherine A. Garcia[1,3], Alyse A. Larkin[1], Nathan S. Garcia[1], Adam J. Fagan[1], and Adam C. Martiny[1,2,*]

[1] Department of Earth System Science, University of California, Irvine, California 92697, USA
[2] Department of Ecology and Evolutionary Biology, University of California, Irvine, California 92697, USA
[3] Center for Microbial Oceanography: Research and Education (C-MORE), University of Hawaii at Manoa, Hawaii, USA
[*] Corresponding author (amartiny@uci.edu)

Supporting Information

Table 1: Surface POM samples from Bio-GO-SHIP cruises used in this study. All POM data used in this study are publicly available. *C13.5 is a partial occupation of the A13.5 GO-SHIP line that was aborted due to COVID-19. See Larkin et al. (2021)[28] for further details on metadata variables.

Campaign	Temporal Coverage	Spatial Coverage	DOI	n
AE1319, NSF	15 August 2013 - 08 September 2013	Western North Atlantic (N:55.0000 E:-40.0100 S:31.6700 W:-69.2100)	https://doi.org/10.26008/1912/bco-dmo.538091.2	16
AMT-28, PML AMT SOCCOM, NSF	25 September 2018 - 27 October 2018	Meridional Atlantic Transect (N:49.6380 E:-5.5020 S: -48.1990 W:-52.692)	https://doi.org/10/fmkq	774
BVAL46, NSF, BATS	28 September 2011 - 12 October 2011	Mid-North Atlantic (N:39.4528 E:-64.1485 S:19.6666 W: -65.9667)	https://doi.org/10.26008/1912/bco-dmo.538091.2	10
C13.5*, GO-SHIP	21 March 2020 – 16 April 2020	Meridional Atlantic Transect (N: 34.5044 E:17.3055 S:-41.4917 W:-73.51)	https://doi.org/10.26008/1912/bco-dmo.868908.1	110
I09N, GO-SHIP	22 March 2016 – 24 April 2016	Eastern Indian Ocean (N:17.8831 E:110.4547 S:-31.0335 W:84.7526)	https://doi.org/10.26008/1912/bco-dmo.734915.3	238
NH1418, NSF	20 September 2014 – 6 October 2014	Tropical Pacific Ocean (N:19.0010 E:-149.6700 S:-3.0001 W:-158.0000)	https://doi.org/10.26008/1912/bco-dmo.829895.1	24
P18, GO-SHIP	13 November 2016 – 28 January 2017	Meridional Pacific Transect (N:28.9071 E:-100.3721 S:-69.9027 W:-116.0561)	https://doi.org/10.26008/1912/bco-dmo.816347.1	198

Table 2: Area-weighted global mean C:N:P (Observation)

	Mean	l-95% CI	u-95% CI	n
C:P	148.4	146.7	150.1	1295
N:P	21.9	21.7	22.2	1295
C:N	6.76	6.72	6.81	1295

Table 3: Area-weighted global mean C:N:P (Observation, binned by 1-by-1 grid)

	Mean	l-95% CI	u-95% CI	n
C:P	147.2	144.7	149.8	460
N:P	21.7	21.4	22.1	460
C:N	6.77	6.7	6.86	460

Table 4: Regionally-binned, area-weighted C:N:P. Polar (|Latitude| ≥ 65°), Subpolar (45° ≤ |Latitude| < 65°), Subtropical (15° ≤ |Latitude| < 45°), and Tropical (|Latitude| < 15°). Mean, and 95% confidence intervals were computed for log-transformed C:N:P ratios and were converted back by taking the exponential.

Region	Mean	Median	l-95% CI	u-95% CI	n
C:P					
Polar	86.1	82.6	63.1	125.3	8
Subpolar	132.6	134.1	65.5	198.0	131
Subtropical	157.6	156.4	91.4	226.4	711
Tropical	139.4	135.4	97.5	187.7	445
N:P					
Polar	15.4	14.3	11.7	21.9	8
Subpolar	21.3	21.5	13.7	28.6	131
Subtropical	22.9	22.7	14.0	31.4	711
Tropical	21.0	20.3	14.5	30.2	445
C:N					
Polar	5.7	5.7	5.2	6.1	8
Subpolar	6.2	6.1	5.0	7.3	131
Subtropical	6.9	6.9	5.0	8.8	711
Tropical	6.7	6.7	5.1	8.5	445

Table 5: Correlation matrix for (Sub)polar region C:N:P, shown in the main Fig. 2a. Asterisks represent the statistical significance (***: $p < 0.001$, **: $p < 0.01$, *: $p < 0.05$, NA: Not Applicable).

	Absolute Latitude	SST	Nitrate	Phosphate	FeT	Nutricline	MLD	MLPAR	Chl-a	% Diatoms	% Cyano
C:P	-0.70 (***)	0.76 (***)	-0.56 (***)	-0.59 (***)	-0.33 (**)	*NA*	0.01	-0.17	0.33 (***)	-0.60 (***)	0.53 (***)
N:P	-0.64 (***)	0.66 (***)	-0.44 (***)	-0.50 (***)	-0.25 (*)	*NA*	-0.03	-0.12	0.31 (***)	-0.48 (***)	0.42 (***)
C:N	-0.27 (**)	0.37 (***)	-0.39 (***)	-0.33 (***)	-0.23 (*)	*NA*	0.10	-0.16	0.09	-0.39 (***)	0.38 (***)

Table 6: Correlation matrix for (Sub)tropical region C:N:P, shown in the main Fig. 2a.

	Absolute Latitude	SST	Nitrate	Phosphate	FeT	Nutricline	MLD	MLPAR	Chl-a	% Diatoms	% Cyano
C:P	0.18 (***)	0.01	-0.33 (***)	-0.25 (***)	-0.09 (*)	0.44 (***)	-0.19 (***)	0.12 (***)	-0.35 (***)	-0.21 (***)	0.34 (***)
N:P	0.20 (***)	-0.14 (***)	-0.09 (**)	-0.11 (***)	-0.11 (**)	0.26 (***)	-0.03	-0.03	-0.13 (***)	0.02	0.10 (***)
C:N	-0.01	0.24 (***)	-0.41 (***)	-0.24 (***)	0.00	0.33 (***)	-0.25 (***)	0.24 (***)	-0.37 (***)	-0.37 (***)	0.40 (***)

Table 7: The individual explained deviance and additive contribution of the four main contextual variables to the total explained deviance in generalized additive models (GAMs) for (Sub)polar region C:N:P as shown in the main Fig. 2b. Asterisks represent the statistical significance (***: $p < 0.001$, **: $p < 0.01$, *: $p < 0.05$).

	SST	Nitrate	Nutricline	Nutricline x Nutlim	Total Explained Deviance
C:P	0.39 (***)	0.24	0	0	0.63
N:P	0.24 (***)	0.26 (***)	0	0	0.50
C:N	0.20 (**)	0.18 (*)	0	0	0.38

Table 8: As in Table 7 but for (Sub)tropical region C:N:P.

	SST	Nitrate	Nutricline	Nutricline x Nutlim	Total Explained Deviance
C:P	0.13 (***)	0.01	0.12 (***)	0.21 (***)	0.47
N:P	0.10 (***)	0.02 (*)	0.07	0.27 (***)	0.46
C:N	0.04 (***)	0.06 (***)	0.01	0.10 (***)	0.22

Table 9: Regionally-binned, area-weighted mean C:P and N:P under the SSP3-7.0 and historic CMIP6 scenarios.

Region	C:P Historical (2010s)	C:P SSP3-7.0 (2090s)	N:P Historical (2010s)	N:P SSP3-7.0 (2090s)
Polar (|Latitude| ≥ 65°)	70.8	76.8	12.9	13.0
Subpolar (45° ≤ |Latitude| < 65°)	101.9	113.3	17.0	18.4
Subtropical (15° ≤ |Latitude| < 45°)	149.2	146.6	21.8	21.5
Tropical (|Latitude| < 15°)	133.4	128.1	19.6	18.2
(Sub)polar (|Latitude| ≥ 45°)	93.5	103.7	16.0	17.0
(Sub)tropical (|Latitude| < 45°)	143.0	139.3	20.9	20.2
Global	128.0	129.1	19.5	19.3

Additional Information on Hierarchical GAM analysis

As the nutrient limitation information is a categorical variable, we first conducted hierarchical GAM analysis using the R package *mgcv* (Wood, 2011)[61] to determine whether the shape of the function itself varies with different nutrient limitations. Based on the initial data exploration, we hypothesized that the response of CNP with respect to the change in nutricline depth varies with respect to the nutrient limitation type and compared with the null model that the responses are the same for all the nutrient limitation types. Following the methodology by Pedersen et al. (2019)[62], we computed root-mean-squared-error (RMSE) and Akaike Information Criterion (AIC) of 6 interactive GAM models (including the control) by comparing model fit with the observation:

1. Model G = A global smoother (shape) for all observations
2. Model GS = Single common smoother plus group-level smoothers that have the same wiggliness
3. Model GI = Single common smoother plus group-level smoothers that have the different wiggliness
4. Model S = Group-specific smoothers (shape) without a global smoother, but all smoothers have the same wiggliness.
5. Model I = Group-specific smoothers with different wiggliness
6. Model C = Control (no group-level smoothers), no nutrient limitation effect

To compare the performance of each model, we conducted *k*-fold cross-validation (100 random partitions holding out 20% of observations) and found that model GS performed best over other models in terms of the RMSE for C:P, N:P, and C:N (Supplementary Figures 1-3) and for AIC (not shown). Thus, we decided to use the model GS to describe the interaction between nutricline and element-specific nutrient limitation throughout this paper. See Extended Data Fig. 3-5 for GAMs with Model GS describing the interaction between nutricline depth and nutrient limitation types.

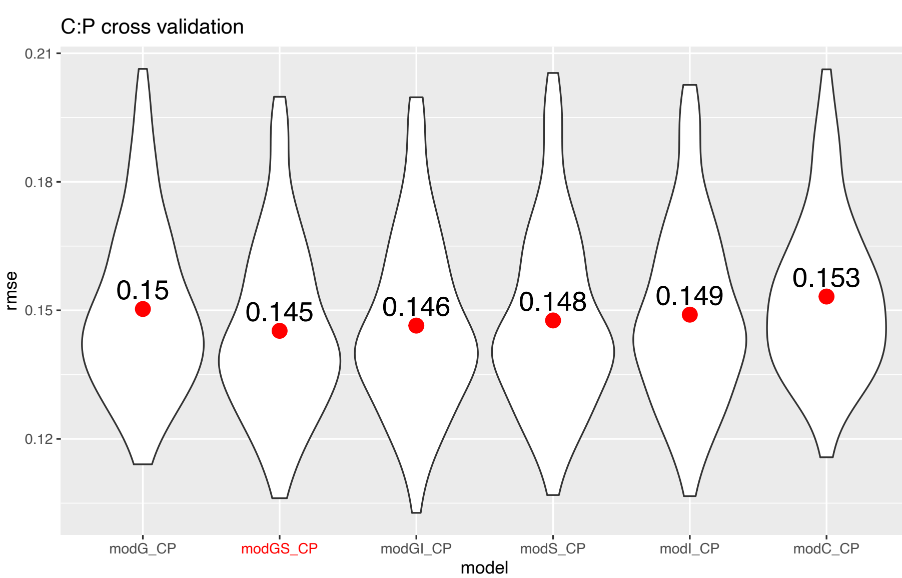

Supplementary Figure 1: Comparison of different hierarchical GAM models describing interaction nutricline and nutrient limitation types for C:P. rmse = Root-Mean-Squared-Error for the fit against observation. Model GS (our model of choice) is highlighted in red.

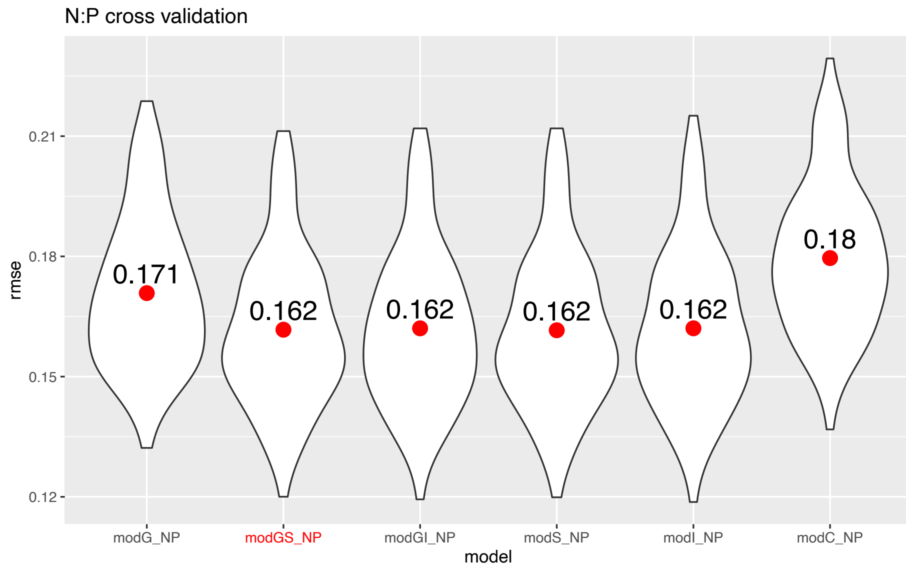

Supplementary Figure 2: Same as Supplementary Figure 1 but for N:P.

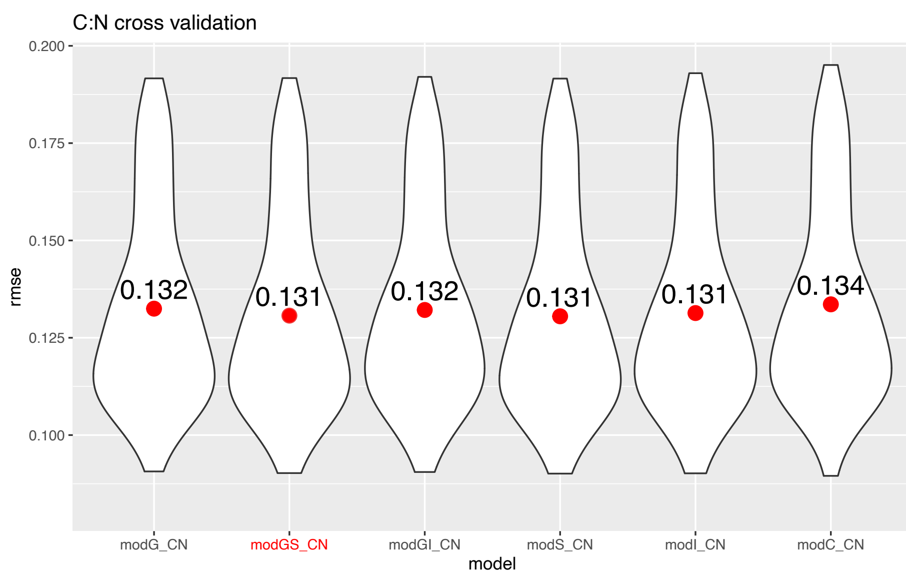

Supplementary Figure 3: Same as Supplementary Figure 1 but for C:N.

References:

1. Redfield, A. C., Ketchum, B. H. & Richards, F. A. The influence of organisms on the composition of Seawater. in *The composition of seawater: Comparative and descriptive oceanography. The sea: ideas and observations on progress in the study of the seas* (ed. Hill, M. N.) vol. 2 26–77 (Interscience Publishers, 1963).
2. Deutsch, C. & Weber, T. Nutrient Ratios as a Tracer and Driver of Ocean Biogeochemistry. *Ann. Rev. Mar. Sci.* **4**, 113–141 (2012).
3. Martiny, A. C. *et al.* Strong latitudinal patterns in the elemental ratios of marine plankton and organic matter. *Nat. Geosci.* **6**, 279–283 (2013).
4. Quay, P. Impact of the Elemental Composition of Exported Organic Matter on the Observed Dissolved Nutrient and Trace Element Distributions in the Upper Layer of the Ocean. *Global Biogeochem. Cycles* **35**, 1–16 (2021).
5. Teng, Y.-C., Primeau, F. W., Moore, J. K., Lomas, M. W. & Martiny, A. C. Global-scale variations of the ratios of carbon to phosphorus in exported marine organic matter. *Nat. Geosci.* **7**, 895–898 (2014).
6. Garcia, C. A. *et al.* Nutrient supply controls particulate elemental concentrations and ratios in the low latitude eastern Indian Ocean. *Nat. Commun.* **9**, 4868 (2018).
7. Singh, A. *et al.* C : N : P stoichiometry at the Bermuda Atlantic Time-series Study station in the North Atlantic Ocean. *Biogeosciences* **12**, 6389–6403 (2015).
8. Karl, D. M. *et al.* Ecological nitrogen-to-phosphorus stoichiometry at station ALOHA. *Deep Sea Res. Part II Top. Stud. Oceanogr.* **48**, 1529–1566 (2001).
9. Fagan, A. J., Moreno, A. R. & Martiny, A. C. Role of ENSO Conditions on Particulate Organic Matter Concentrations and Elemental Ratios in the Southern California Bight. *Front. Mar. Sci.* **6**, 386 (2019).
10. Matsumoto, K., Tanioka, T. & Rickaby, R. Linkages Between Dynamic Phytoplankton C:N:P and the Ocean Carbon Cycle Under Climate Change. *Oceanography* **33**, 44–52 (2020).
11. Galbraith, E. D. & Martiny, A. C. A simple nutrient-dependence mechanism for predicting the stoichiometry of marine ecosystems. *Proc. Natl. Acad. Sci.* **112**, 8199–8204 (2015).
12. Wang, W.-L., Moore, J. K., Martiny, A. C. & Primeau, F. W. Convergent estimates of marine nitrogen fixation. *Nature* **566**, 205–211 (2019).
13. Mills, M. M. & Arrigo, K. R. Magnitude of oceanic nitrogen fixation influenced by the nutrient uptake ratio of phytoplankton. *Nat. Geosci.* **3**, 412–416 (2010).
14. Kwiatkowski, L., Aumont, O., Bopp, L. & Ciais, P. The Impact of Variable Phytoplankton Stoichiometry on Projections of Primary Production, Food Quality, and Carbon Uptake in the Global Ocean. *Global Biogeochem. Cycles* **32**, 516–528 (2018).
15. Sterner, R. W. & Elser, J. J. *Ecological stoichiometry: the biology of elements from molecules to the biosphere*. (Princeton University Press, 2002).
16. Allen, A. P. & Gillooly, J. F. Towards an integration of ecological stoichiometry and the metabolic theory of ecology to better understand nutrient cycling. *Ecol. Lett.* **12**, 369–384 (2009).
17. Moreno, A. R. & Martiny, A. C. Ecological Stoichiometry of Ocean Plankton. *Ann. Rev. Mar. Sci.* **10**, 43–69 (2018).
18. Schaum, C.-E., Buckling, A., Smirnoff, N., Studholme, D. J. & Yvon-Durocher, G. Environmental fluctuations accelerate molecular evolution of thermal tolerance in a marine diatom. *Nat. Commun.* **9**, 1719 (2018).

19. Geider, R. & La Roche, J. Redfield revisited: variability of C:N:P in marine microalgae and its biochemical basis. *Eur. J. Phycol.* **37**, 1–17 (2002).
20. Sharoni, S. & Halevy, I. Nutrient ratios in marine particulate organic matter are predicted by the population structure of well-adapted phytoplankton. *Sci. Adv.* **6**, eaaw9371 (2020).
21. Bonachela, J. A., Klausmeier, C. A., Edwards, K. F., Litchman, E. & Levin, S. A. The role of phytoplankton diversity in the emergent oceanic stoichiometry. *J. Plankton Res.* **38**, 1021–1035 (2016).
22. Quigg, A. *et al.* The evolutionary inheritance of elemental stoichiometry in marine phytoplankton. *Nature* **425**, 291–4 (2003).
23. Yvon-Durocher, G., Dossena, M., Trimmer, M., Woodward, G. & Allen, A. P. Temperature and the biogeography of algal stoichiometry. *Glob. Ecol. Biogeogr.* **24**, 562–570 (2015).
24. Martiny, A. C. *et al.* Biogeochemical controls of surface ocean phosphate. *Sci. Adv.* **5**, eaax0341 (2019).
25. Moore, C. M. *et al.* Processes and patterns of oceanic nutrient limitation. *Nat. Geosci.* **6**, 701–710 (2013).
26. Klausmeier, C. A., Litchman, E. & Levin, S. A. Phytoplankton growth and stoichiometry under multiple nutrient limitation. *Limnol. Oceanogr.* **49**, 1463–1470 (2004).
27. Garcia, N. S., Bonachela, J. A. & Martiny, A. C. Interactions between growth-dependent changes in cell size, nutrient supply and cellular elemental stoichiometry of marine Synechococcus. *ISME J.* **10**, 1–10 (2016).
28. Larkin, A. A. *et al.* High spatial resolution global ocean metagenomes from Bio-GO-SHIP repeat hydrography transects. *Sci. Data* **8**, 107 (2021).
29. Clayton, S. *et al.* Bio-GO-SHIP: The Time Is Right to Establish Global Repeat Sections of Ocean Biology. *Front. Mar. Sci.* **8**, (2022).
30. Martiny, A. C., Vrugt, J. A., Primeau, F. W. & Lomas, M. W. Regional variation in the particulate organic carbon to nitrogen ratio in the surface ocean. *Global Biogeochem. Cycles* **27**, 723–731 (2013).
31. Ustick, L. J. *et al.* Metagenomic analysis reveals global-scale patterns of ocean nutrient limitation. *Science (80-.).* **372**, 287–291 (2021).
32. Richardson, K. & Bendtsen, J. Vertical distribution of phytoplankton and primary production in relation to nutricline depth in the open ocean. *Mar. Ecol. Prog. Ser.* **620**, 33–46 (2019).
33. Cermeno, P. *et al.* The role of nutricline depth in regulating the ocean carbon cycle. *Proc. Natl. Acad. Sci.* **105**, 20344–20349 (2008).
34. Toseland, A. *et al.* The impact of temperature on marine phytoplankton resource allocation and metabolism. *Nat. Clim. Chang.* **3**, 979–984 (2013).
35. Sauterey, B. & Ward, B. A. Environmental control of marine phytoplankton stoichiometry in the North Atlantic Ocean. *Proc. Natl. Acad. Sci.* **119**, e2114602118 (2022).
36. Marañón, E., Lorenzo, M. P., Cermeño, P. & Mouriño-Carballido, B. Nutrient limitation suppresses the temperature dependence of phytoplankton metabolic rates. *ISME J.* **12**, 1836–1845 (2018).
37. Thomas, M. K. *et al.* Temperature–nutrient interactions exacerbate sensitivity to warming in phytoplankton. *Glob. Chang. Biol.* **23**, 3269–3280 (2017).
38. Droop, M. R. The nutrient status of algal cells in continuous culture. *J. Mar. Biol. Assoc. United Kingdom* **54**, 825–855 (1974).

39. Hillebrand, H. *et al.* Goldman revisited: Faster growing phytoplankton has lower N:P and lower stoichiometric flexibility. *Limnol. Oceanogr.* **58**, 2076–2088 (2013).
40. Barton, S. *et al.* Evolutionary temperature compensation of carbon fixation in marine phytoplankton. *Ecol. Lett.* **23**, 722–733 (2020).
41. Weber, T. S. & Deutsch, C. Oceanic nitrogen reservoir regulated by plankton diversity and ocean circulation. *Nature* **489**, 419–422 (2012).
42. Gruber, N. & Sarmiento, J. L. Global patterns of marine nitrogen fixation and denitrification. *Global Biogeochem. Cycles* **11**, 235–266 (1997).
43. Moore, J. K., Doney, S. C. & Lindsay, K. Upper ocean ecosystem dynamics and iron cycling in a global three-dimensional model. *Global Biogeochem. Cycles* **18**, (2004).
44. Cael, B. B., Dutkiewicz, S. & Henson, S. A. Abrupt shifts in 21st-century plankton communities. *Sci. Adv.* **7**, 8593–8622 (2021).
45. Penuelas, J., Janssens, I. A., Ciais, P., Obersteiner, M. & Sardans, J. Anthropogenic global shifts in biospheric N and P concentrations and ratios and their impacts on biodiversity, ecosystem productivity, food security, and human health. *Glob. Chang. Biol.* **26**, 1962–1985 (2020).
46. Jiang, H.-B. *et al.* Ocean warming alleviates iron limitation of marine nitrogen fixation. *Nat. Clim. Chang.* **8**, 709–712 (2018).
47. Krishnamurthy, A., Moore, J. K., Mahowald, N., Luo, C. & Zender, C. S. Impacts of atmospheric nutrient inputs on marine biogeochemistry. *J. Geophys. Res.* **115**, G01006 (2010).
48. Talarmin, A. *et al.* Seasonal and long-term changes in elemental concentrations and ratios of marine particulate organic matter. *Global Biogeochem. Cycles* **30**, 1699–1711 (2016).
49. Tanioka, T., Fichot, C. G. & Matsumoto, K. Toward Determining the Spatio-Temporal Variability of Upper-Ocean Ecosystem Stoichiometry From Satellite Remote Sensing. *Front. Mar. Sci.* **7**, 604893 (2020).
50. Garcia, C. A. *et al.* Linking regional shifts in microbial genome adaptation with surface ocean biogeochemistry. *Philos. Trans. R. Soc. B Biol. Sci.* **375**, 20190254 (2020).
51. Lee, J. A., Garcia, C. A., Larkin, A. A., Carter, B. R. & Martiny, A. C. Linking a Latitudinal Gradient in Ocean Hydrography and Elemental Stoichiometry in the Eastern Pacific Ocean. *Global Biogeochem. Cycles* **35**, (2021).
52. Lomas, M. W. *et al.* Sargasso Sea phosphorus biogeochemistry: An important role for dissolved organic phosphorus (DOP). *Biogeosciences* **7**, 695–710 (2010).
53. Becker, S. *et al.* GO-SHIP Repeat Hydrography Nutrient Manual: The Precise and Accurate Determination of Dissolved Inorganic Nutrients in Seawater, Using Continuous Flow Analysis Methods. *Front. Mar. Sci.* **7**, 908 (2020).
54. Lauvset, S. K. *et al.* A new global interior ocean mapped climatology: the 1° × 1° GLODAP version 2. *Earth Syst. Sci. Data* **8**, 325–340 (2016).
55. Key, R. M. *et al. Global ocean data analysis project, version 2 (GLODAPv2). Ornl/Cdiac-162, Ndp-093* (2015) doi:10.3334/CDIAC/OTG.NDP093_GLODAPv2.
56. Brun, P. *et al.* Ecological niches of open ocean phytoplankton taxa. *Limnol. Oceanogr.* **60**, 1020–1038 (2015).
57. Holte, J., Talley, L. D., Gilson, J. & Roemmich, D. An Argo mixed layer climatology and database. *Geophys. Res. Lett.* **44**, 5618–5626 (2017).
58. Gregg, W. W. & Casey, N. W. Sampling biases in MODIS and SeaWiFS ocean chlorophyll data. *Remote Sens. Environ.* **111**, 25–35 (2007).

59. Gregg, W. W., Ginoux, P., Schopf, P. S. & Casey, N. W. Phytoplankton and iron: validation of a global three-dimensional ocean biogeochemical model. *Deep Sea Res. Part II Top. Stud. Oceanogr.* **50**, 3143–3169 (2003).
60. R Core Team. R: A Language and Environment for Statistical Computing. (2021).
61. Wood, S. N. Fast stable restricted maximum likelihood and marginal likelihood estimation of semiparametric generalized linear models. *J. R. Stat. Soc. Ser. B Stat. Methodol.* **73**, 3–36 (2011).
62. Pedersen, E. J., Miller, D. L., Simpson, G. L. & Ross, N. Hierarchical generalized additive models in ecology: An introduction with mgcv. *PeerJ* **2019**, (2019).
63. Rodgers, K. *et al.* Ubiquity of human-induced changes in climate variability. *Earth Syst. Dyn. Discuss.* 1–22 (2021) doi:10.5194/ESD-2021-50.
64. O'Neill, B. C. *et al.* A new scenario framework for climate change research: the concept of shared socioeconomic pathways. *Clim. Change* **122**, 387–400 (2014).